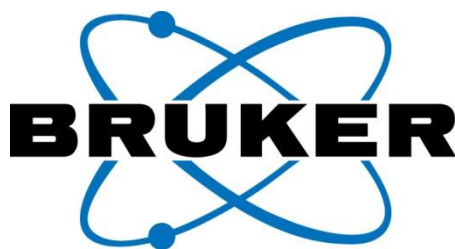


23rd Benelux EPR Society Meeting

Ghent, May 22nd 2015



Sponsored by Bruker

Organizing committee from Ghent University

Organizers: Henk Vrielinck and Freddy Callens

Secretary: Irena Nevjestić

Other members: Kristof Daelman, Nico De Roo, Jevgenij Kusakovskij, Wouter Leroy, Kwinten Maes, Johan Van Driessche

23rd Benelux EPR Society Meeting – Program

10:00 Registration

10:25 Opening

Session 1

10:30 – Irena Nevjestić (Ghent University)

‘EPR and ENDOR study of a V-doped Al-metal organic framework’

10:50 – Elena Morra (University of Antwerp)

‘EPR techniques applied to the study of Ziegler-Natta catalysts’

11:10 – Nicholas Cox (Max Planck Institute for Chemical Energy Conversion - Mülheim)

‘The structure of nature’s water splitting catalyst prior to O-O bond formation as determined by W-band EPR’

11:30 Coffee break

Session 2

11:45 – Manuela Liberi (Bruker)

‘Bruker EMXnano: the New High-Performance Benchtop EPR System’

12:05 – Fred Hagen (Delft University of Technology)

‘0-18 GHz broadband transmission cw-EPR; a progress report’

12:25 Lunch break + Poster session

Session 3

14:30 – Mouithys-Mickalad Ange (University of Liège)

‘Modulatory effects of Ruthenium(II)-based complexes on oxidative stress induced by activated HL60 cells and Neutrophils’

14:50 – Céline Desmet (Université Catholique de Louvain – Brussels)

‘Monitoring of tissue oxygenation during wound healing in diabetic models’

15:10 – Ernst van Faassen (LUMC Leiden)

‘EPR investigation of kidney function in diabetic albuminuria’

15:30 Coffee break

Session 4

15:50 – Mykhailo Azarkh (Leiden University)

‘Grid-of-errors: a numerical procedure to extract the distribution of magnetic interactions from multi-frequency EPR spectra’

16:10 – Martina Huber (Leiden University)

‘Internal structure of Amyloid-fibrils from EPR long-range distance constraints – possibilities and challenges’

16:30 General meeting of the Benelux EPR Society

16:45 Reception + Poster session

Poster session

P1 – Flavia Deizotti (Université Catholique de Louvain – Brussels)

‘Impact of erythrocytic eNOS on HbNO formation measured by EPR spectroscopy’

P2 – Gauthier Vanhaelewyn (Ghent University)

‘Preliminary EPR results of the influence of storage temperature on the endogenous antioxidative potential of a widely distributed Belgian pale lager beer’

P3 – Gabriele Panarelli (Leiden University)

‘Multi-frequency EPR spectroscopy of Eu^{2+} –activated persistent luminescent materials’

P4 – Bert Cuypers (University of Antwerp)

‘Characterization of Class 1 hemoglobins from the model legume *Lotus japonicus* using EPR and optical spectroscopy’

P5 – Serena Iacovo (University of Leuven)

‘Processing-induced near-interfacial thermal donor generation in (100)Si/Si-oxycarbide insulator structures revealed by electron spin resonance’

P6 – Shashi K. R. Singam (University of Antwerp)

‘Effect of laser excitation intensity on the spin-dependent NV⁻ fluorescence in diamond’

P7 - Simon Collienne (University of Liège)

‘Electron paramagnetic resonance and fluorescence studies on potential anticancer properties of two new Ru(II) complexes : preliminary results’

P8 – Jevgenij Kusakovskij (Ghent University)

‘Electron magnetic resonance study of radiation-induced radicals in DNA’

Abstracts Oral Presentations

EPR and ENDOR study of a V-doped Al-metal organic framework

Irena Nevjestić^{*1}, Hannes Depauw², Karen Leus², Vidmantas Kalendra^{3,4}, Ignacio Caretti⁵, Gunnar Jeschke³, Sabine Van Doorslaer⁵, Freddy Callens¹, Pascal Van Der Voort² and Henk Vrielinck¹

¹Ghent University, Dept. of Solid State Sciences, Krijgslaan 281-S1, B-9000 Gent, Belgium, *Irena.Nevjestic@UGent.be

²Ghent University, Dept. of Inorganic and Physical Chemistry, COMOC, Krijgslaan 281-S3, B-9000 Gent, Belgium

³ETH Zürich, Vladimir-Prelog-Weg 2, CH-8093 Zürich, Switzerland

⁴Faculty of Physics, Vilnius University, Sauletekio av. 9, LT-10222 Vilnius, Lithuania

⁵University of Antwerp, Campus Drie Eiken, Universiteitsplein 1, 2610 Wilrijk, Belgium

Metal-Organic Frameworks (MOFs) are ordered porous materials constructed of metal ions connected by organic linkers. These materials possess many interesting features, like well-defined pore size, pore shape and ultra-high porosity. A characteristic example of MOFs with one dimensional pores is MIL-53 ([Al(OH)(BDC), BDC = terephthalate or 1,4-benzenedicarboxylate]. The 3D framework of as-synthesized MIL-53 is built up of infinite chains of corner-sharing $\text{AlO}_4(\text{OH})_2$ octahedra with BDC connecting these chains. The 1D channels are filled with disordered uncoordinated terephthalic acid molecules and other impurities, which can be removed by calcination or solvent extraction methods, which are referred to as activation procedures. After activation MIL-53 exhibits breathing: the framework can reversibly change from a large pore (lp) to narrow pore (np) structure by changing temperature or pressure.

EPR and ENDOR spectroscopy are excellent tools for characterizing V^{IV} -centers (with a $3d^1$ electron configuration) in MIL-53. The EPR spectra of as-synthesized V-doped MIL-53 show nicely resolved ^{51}V ($I=7/2$) hyperfine (HF) structure. The spectra at RT are dominated by a center with rhombic g and ^{51}V HF tensors whose principal axes do not coincide. ENDOR spectra reveal interaction with the central ^{51}V , ^{27}Al ($I=5/2$) and ^1H ($I=1/2$) nuclei, suggesting that vanadyl ions substitute Al-OH in the MIL-53 framework.

The EPR spectra of activated V-doped MIL-53 differ from those of as-synthesized MIL-53. Furthermore, the EPR spectra of V^{IV} in the large and narrow pore forms of MIL-53 can easily be distinguished (Figure 1). ENDOR spectra (10 K, narrow pore) reveal interactions with the same types of nuclei as in as-synthesized V-doped MIL-53 in a slightly different coordination environment.

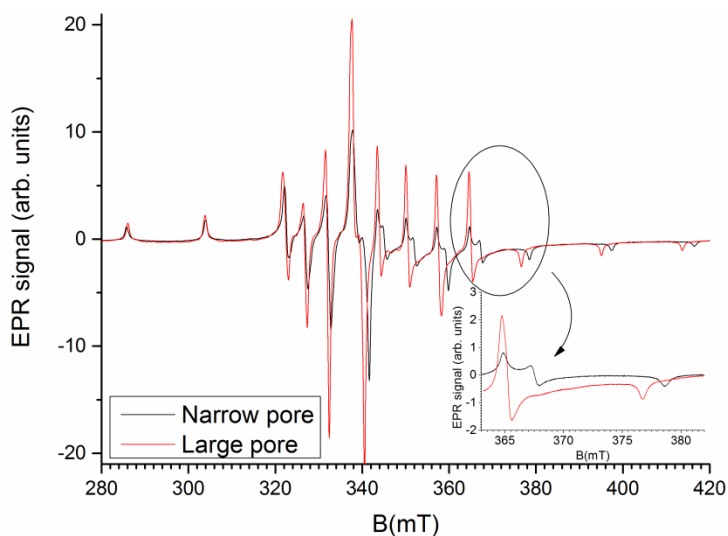


Figure 1 - EPR spectra of V-doped MIL-53 at RT in X-band (9.5 GHz). Black spectrum – narrow pore form, red spectrum – large pore form. Inset shows enlarged part of the spectrum where differences between np and lp form spectra are evident.

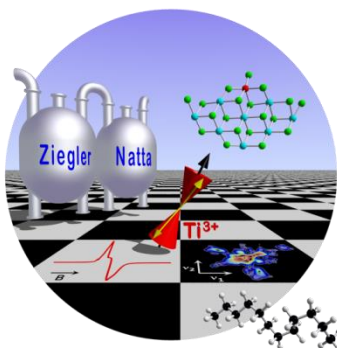
EPR techniques applied to the study of Ziegler-Natta catalysts

E. Morra^(a,b,c), M. Chiesa^(a), S. Van Doorslaer^(b)

(a) Dipartimento di Chimica, Università degli Studi di Torino, Via Giuria 7, 10125 Torino, Italy

(b) Department of Physics, University of Antwerp, Universiteitsplein 1, B-2610 Antwerp-Wilrijk, Belgium

(c) Dutch Polymer Institute (DPI), P.O. Box 902, 5600 AX Eindhoven, The Netherlands



Abstract

In this work, multi-frequency (X-, Q-, W-band) continuous wave and pulse EPR techniques are applied for investigating Ti^{3+} species in high-yield Ziegler-Natta catalysts (HY-ZNCs). HY-ZNCs are MgCl_2 -supported Ti-based heterogeneous catalysts employed for the industrial production of polyethylene and polypropylene. Upon activation with an alkyl aluminum co-catalyst, Ti^{3+} species are generated which are believed to play a central role in Ziegler-Natta catalysis. Due to the paramagnetic nature of Ti^{3+} (d^1 , $S=1/2$), EPR spectroscopy is a method of choice for investigating these species, however its applications in this field are quite limited considering that only X-band CW EPR has been exploited so far. Modern EPR techniques can thus provide new insights into the geometric and electronic structure of potentially active Ti^{3+} sites in HY-ZNCs.

In view of the complexity and multi-component nature of the HY-ZNCs, a bottom-up approach of investigation is exploited. Model systems of increasing complexity are considered, ranging from Ti-chloride homogeneous solutions [1] to close-to-real MgCl_2 -supported systems.

Particular attention will be given to the EPR characterization of an industrial HY-ZNC [2]. Two main families of isolated molecular-like Ti^{3+} species have been identified. The reactivity of the catalyst was tested against oxygen as a probe molecule, leading to the formation of superoxide O_2^- radical anions stabilized on particular Ti sites and whose surrounding was monitored through pulse EPR experiments.

References

- [1] S. Maurelli, E. Morra, S. Van Doorslaer, V. Busico, M. Chiesa, *Phys. Chem. Chem. Phys.* **2014**, 16, 19625-19633.
- [2] E. Morra, E. Giamello, S. Van Doorslaer, G. Antinucci, M. D'Amore, V. Busico, M. Chiesa, *Angew. Chem.* **2015**, 54, 4857-4860.

This work is part of the research program of the Dutch Polymer Institute (DPI), project nr. 754.

The structure of nature's water splitting catalyst prior to O-O bond formation as determined by W-band EPR

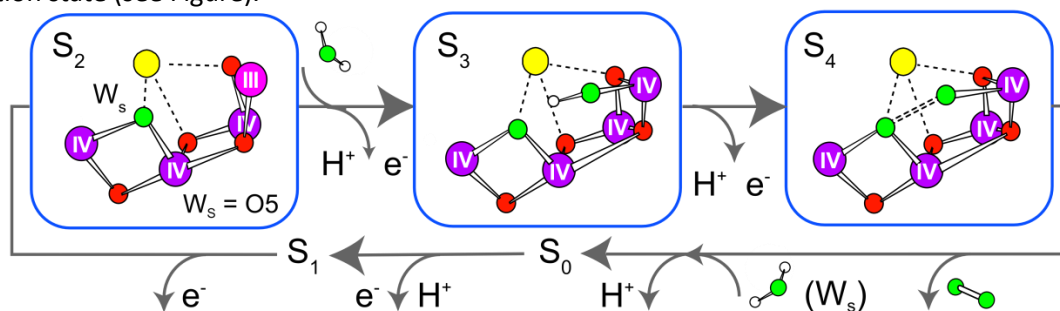
Nicholas Cox,¹ Marius Retegan,¹ Frank Neese,¹ Alain Boussac,² Dimitrios A. Pantazis,¹ Wolfgang Lubitz¹

¹Max Planck Institute for Chemical Energy Conversion, D-45470 Mülheim (Ruhr) Germany

²iBiTec-S, CNRS UMR 8221, CEA Saclay, 91191 Gif-sur-Yvette, France

E-mail: nicholas.cox@cec.mpg.de

Pulse W-band EPR data are reported for the last metastable intermediate of nature's water splitting catalyst.¹ The catalyst represents a penta-oxygen, tetramanganese-calcium cofactor.^{2,3} Simulations of the entire EPR dataset using the spin Hamiltonian formalism require this intermediate to have a ground electronic state of $S = 3$ and exhibit a small fine structure splitting ($|D| < 0.2 \text{ cm}^{-1}$), consistent with the cofactor representing an all Mn^{IV} complex in this state.¹ Concomitant double resonance measurements (ELDOR-detected NMR) support this assignment. These measurements allow all manganese nuclear transition of the cofactor to be simultaneously visualized, over the 10-300 MHz range with high sensitivity, allowing the Mn ions that constitute the water splitting catalyst to be examined independently.¹ It is observed that all four Mn ions of the catalyst are structurally and electronically similar in the last intermediate state: they all have the same formal oxidation state of IV+ and an octahedral local geometry ($t_g^3 e_g^0$).¹ These results are interpreted with the aid of density functional theory calculations. It is shown that only one structural model is consistent with all magnetic resonance data.¹⁻⁴ This model requires the binding of an additional water molecule, possibly the second substrate water, to the manganese cofactor during the formation of the last intermediate^{1,5} and assign its binding position. These new experiments resolve the mechanism of the biological water splitting reaction, with the O-O bond forming between two manganese bound oxygens in the transition state (see Figure).^{1,6}



References

- [1] Cox N., Retegan M., Neese F., Pantazis D.A., Boussac A., Lubitz W., Electronic structure of the oxygen-evolving complex in photosystem II prior to O-O bond formation, *Science* **2014**, 345, 804-808
- [2] Cox, N., Pantazis, D.A., Neese, F., Lubitz, W., Biological water oxidation *Acc. Chem. Res.*, **2013** 46, 1588.
- [3] Umena, Y., Kawakami, K., Shen, J.-R., Kamiya, K., Crystal structure of oxygen-evolving photosystem II at a resolution of 1.9 Å, *Nature* **2011** 473, 55
- [4] Pantazis, D. A.; Ames, W.; Cox, N.; Lubitz, W.; Neese, F. Two Interconvertible Structures that Explain the Spectroscopic Properties of the Oxygen-Evolving Complex of Photosystem II in the S_2 State, *Angew. Chem. Int. Ed.* **2012** 51, 9935
- [5] Cox, N.; Messinger, J., Reflections on substrate water, *Biochim. Biophys. Acta* **2013**, 1827, 1020
- [6] Siegbahn P.E.M, Structures and Energetics for O_2 Formation in Photosystem II, *Acc. Chem. Res.*, **2009**, 42, 1871-1880

Bruker EMXnano: the new high-performance benchtop EPR system

Manuela Liberi, Bruker Italia, BioSpin Business Unit

Extending the EMX line of spectrometers, Bruker has recently introduced the **EMXnano™**. With its high performance and compact design, the benchtop EPR instrument **EMXnano** makes research-grade EPR accessible to a broader range of scientists.

The **EMXnano** is a full range X-Band EPR spectrometer that can be used to analyze various EPR samples, including transition metals, antioxidants and free radicals. This allows one to gain valuable information and insights into biological and chemical systems. With the SpinCount module, the **EMXnano** provides a reliable tool for quantitative EPR. A combination of simulation via SpinFit and quantitation via SpinCount aids in the identification and interpretation of spin trap adducts.

The **EMXnano** has been designed with the user in mind, delivering research performance with ease of use. The instrument includes defined workflows for easy and fast spectrum acquisition, with a user-friendly interface that allows parameters to be easily adjusted even by non-experts. Various accessories are available to tailor the **EMXnano** to specific application fields.

0-18 GHz broadband transmission cw-EPR; a progress report

Wilfred R Hagen

*Delft University of Technology, Department of Biotechnology, Julianalaan 67, 2628BC Delft,
The Netherlands. w.r.hagen@tudelft.nl*

We develop a cw-EPR transmission spectrometer that is continuously tunable over a wide range of frequencies. While in our previous work we reported on the extension of our original 0-2.7 GHz design [Hagen (2013)PLOS ONE 8 (3) 15p, e59874] to 0-6 GHz, we have now build a frequency-range extender (FRE) to cover 0-18.5 GHz. This choice is based on our view that cw-EPR on biological samples in this frequency range will be practical to unequivocally analyze hyperfine interactions of metal centers and dipolar interactions between different centers in proteins. The FRE is based on switchable broadband doublers in combination with a matching circuit, a broadband amplifier, and a divide-by-four divider.

We use stripline cells that take a sample volume comparable to that of regular X-band samples. Since the cells are (almost) non-resonant we have a sensitivity issue that we attempt to solve by developing a wide-field rapid-scan unit. In our previous work we reported this approach to be practical for scans of limited range of the order of 100 gauss. Preliminary results of attempts to increase this to several thousand gauss will be discussed.

For the static field we use a Bruker B-MN 90/30 electromagnet refurbished with a Danfysik precision power supply that drives the magnet directly without feedback from a Hall probe.

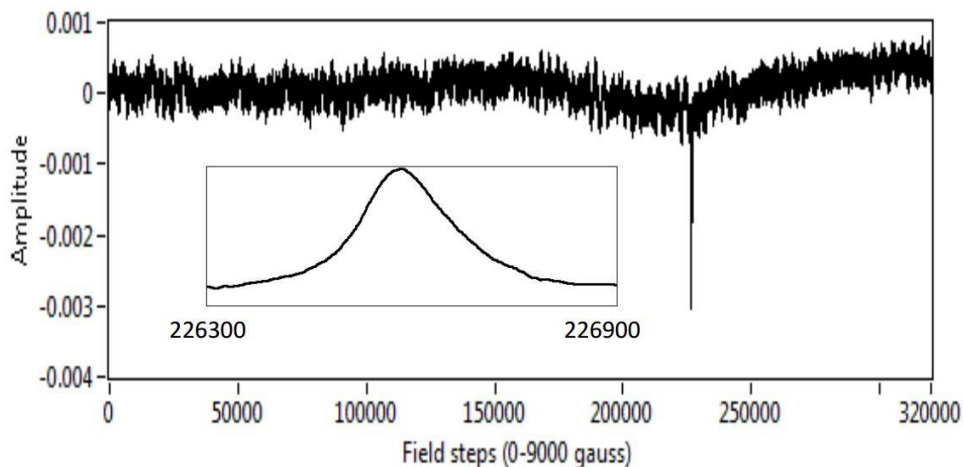


Figure 1. A 17.600000 GHz spectrum of DPPH recorded slowly (300 s) over a 0-9000 gauss field range with 320,000 steps in the magnetic field. The inset is a zoom-in taken directly from the wide scan spectrum.

Modulatory effects of Ruthenium(II)-based complexes on oxidative stress induced by activated HL60 cells and Neutrophils

Collienne S^{1,2}, Franck T^{1,3}, Delaude L⁴, Vaesen F¹, Mormoen J¹, Hoebeke M^{1,2}, Serteyn D^{1,3}, Mouithys-Mickalad A¹

¹ Centre for Oxygen, R&D (CORD), Institute of Chemistry, B6a. ² Laboratory of Biomedical Spectroscopy, Department of Physics, Institute of Physics B5a. ³ Equine Clinic, Faculty of Veterinary Medicine. ⁴ Laboratory of Organometallic Chemistry and Homogeneous Catalysis, Institute of Chemistry, B6a, University of Liège, B-4000 Liège, Belgium.

There is a growing interest in the use of metal-based chemotherapeutic agents to fight different types of cancers [1]. Among the most commonly used family of organometallic compounds derived from platinum, Cisplatin (CisPt) is the lead compound for the treatment of various cancers including lung, testis, gastric, breast, etc. Nevertheless, beside its recognized therapeutic effects, side effects such as gastric toxicity and acute kidney failure were observed during treatment with CisPt, thereby limiting its clinical use. Other compounds are currently studied and among them, Ruthenium (Ru) complexes have gained more importance for their lower toxicity and aggressive effect on healthy tissues than CisPt. Ru-complexes are also more resorbed and excreted [2]. Numerous studies focused on the mechanisms of action of Ruthenium compounds to fight cancer, including antioxidant or pro-oxidant activity.

During inflammation, activation and infiltration of neutrophils contribute to oxidant stress playing a crucial role in tumor development. Likewise, the degranulation of neutrophil causes the release of myeloperoxidase (MPO), which reacts with H₂O₂ to catalyze redox reactions. A therapeutic target to control inflammation is the modulation of oxidant enzymes and cells involved in radical species production and redox reactions.

Because Ruthenium compounds can easily enter into cancer cells, a series of newly synthesized Ru(II)-complexes were used for this purpose. They were first tested for their radical scavenging activities using ABTS and 1,1-diphenyl-2-picrylhydrazyl (DPPH) assays.

Amongst them, compound **1** (LD0436) and compound **2** (LD04037) were then studied for their ability to modulate the reactive oxygen species (ROS) production by inflammatory cells like human promyelocytic leukemia cell line (HL 60) and neutrophils (PMN) using fluorescence, chemiluminescence (CL) and electron spin resonance (ESR) techniques. The toxicity of those Ru-complexes against HL-60 and neutrophils was checked using Trypan blue exclusion assay.

Altogether, CL and ESR findings indicate that both complexes **1** (LD0436) and **2** (LD0437) exhibit a dose-dependent inhibitory activity compared to CisPt, gallic acid, curcumin and quercetin, which were taken as reference molecules in the various systems investigated. Similarly, the Ru(II) complexes tested also display an antioxidant profile on the substrate oxidation catalyzed by peroxidase such as MPO mainly involved in acute and chronic inflammatory situations.

1: (RuCl(*p*-cymene)(S₂C.IDip)]⁺(PF₆)⁻], **2:** (RuCl(*p*-cymene)(S₂C.ICy)]⁺(PF₆)⁻]

References:

1. Ceresa C, Brawin A, Cavaletti G, Trinidad A et al., (2014) Current Medicinal Chemistry 20(21), 2237-2265.
2. Liu, Y, Zhang X, Zhang R, et al., (2011) European Journal of Inorganic Chemistry. 1974-1980.

Monitoring of tissue oxygenation during wound healing in diabetic models

C. Desmet¹, A. Lafosse^{2,3}, S. Vériter², K.K. Cheretty⁴, G. Vandermeulen⁴, P. Porporato⁵, P. Sonveaux⁵, V. Pr at⁴, D. Dufrane², Ph. Lev eque¹, B. Gallez¹

(1) Biomedical Magnetic Resonance Research group, Louvain Drug Research Institute, Universit  catholique de Louvain, Brussels, Belgium

(2) Endocrine Cell Therapy Unit, Center of Tissue/Cell Therapy, Cliniques Universitaires Saint-Luc, Universit  catholique de Louvain, Brussels, Belgium

(3) Plastic and Reconstructive Surgery Unit, Cliniques Universitaires Saint-Luc, Universit  catholique de Louvain, Brussels, Belgium

(4) Advanced Drug Delivery & Biomaterials Research group, Louvain Drug Research Institute, Universit  catholique de Louvain, Brussels, Belgium

(5) Pole of Pharmacology and Therapeutics, Institut de Recherche Exp rimental et Clinique, Universit  catholique de Louvain, Brussels, Belgium

Development of skin ulcers with impaired healing is a common complication of diabetes affecting more than 15% of diabetic patients. Tissue ischemia is a likely cause of wound healing impairments as oxygen plays a key role in wound healing. But to date, the variation of the pO_2 in a wound remains uncertain as there still lacks non invasive methods for absolute and repeated pO_2 measurements in situ. EPR oximetry is a technique that allows repeated measurements of the absolute tissue pO_2 . This technique is based on the measurement of the linewidth of the EPR signal recorded with a biocompatible oxygen sensor like crystals of lithium phtalocyanine (LiPc) implanted in the tissue.

The aim of this work was to study the role of oxygen during wound healing in chronic diabetes models using EPR oximetry.

For this purpose, we tested two wound models in db/db mice (type II diabetes model): a full-thickness excisional skin wound and a pedicled skin flap wound. LiPc crystals were implanted at different wound sites and EPR spectra were recorded repeatedly during wound healing using a L-Band spectrometer (Magnettech, Germany). Measurements were also recorded in diabetic wounds after proangiogenic treatments administration (electroporation of a plasmid encoding VEGF and injection of VEGF encapsulated in PLGA nanoparticles).

The main conclusions of the study are:

- EPR oximetry provides pO_2 measurements during wound healing process.
- 12 weeks-old db/db mice with proven long-term hyperglycemia exhibit microvascular abnormalities and delayed wound healing.
- Pedicled flap wound recapitulates the expected hypoxia at the beginning of the wound healing process contrarily to open wounds (fig. 1).
- Two VEGF treatments tested (electroporation & PLGA based-nanoparticles) had no effect on the reoxygenation and the healing rate of chronic diabetic wounds (fig.2).

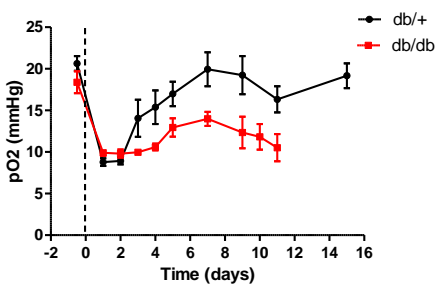


Fig. 1: pO_2 (mmHg) variations in the pedicled skin flap during wound healing in db/+ and db/db mice.

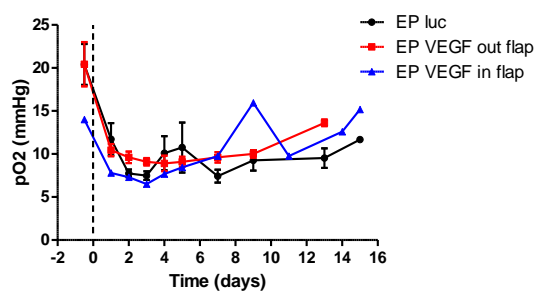


Fig 2: pO_2 (mmHg) variations in the pedicled skin flap in db/db mice after VEGF treatment (plasmid electroporation).

EPR investigation of kidney function in diabetic albuminuria

Ernst van Faassen, Margien Boels,
Bernard van de Berg, Ton Rabelink,
Nephrology Dept, LUMC Leiden
The Netherlands

Currently, detection of free nitric oxide (NO) radicals in living tissues is only possible with NO-spin trapping with iron-dithiocarbamate complexes [1], and detection of the ensuing nitrosylated adducts (paramagnetic $S=1/2$) with EPR spectroscopy. We apply this method to study the nitric oxide status of kidney tissues in a mouse model for diabetic nephropathy.

Pro-diabetes now affects ca 30 % of the population, slowly progressing into manifest diabetes with chronic kidney dysfunction at later stages. It presents with a characteristic failure of the glomerular barrier in the kidney (albuminuria). Proper barrier function is acutely impaired by inhibition of endogenous NO production [2].

Hypothesis: Previously, the endothelin-A receptor antagonist Atrasentan has been shown to reduce albuminuria in diabetic humans, but the mechanism is not understood. We propose that Atrasentan acts by restoring damaged and dysfunctional glycocalyx in the diabetic kidney and improving the NO status.

Mouse model: apoE-KO mice, a mutant particularly prone to high blood cholesterol and atherosclerosis, were rendered diabetic by chronic (12 wks) administration of streptozotocin, followed by 4 wks treatment with Atrasentan or placebo. The mice were tested for renal glycocalyx and albuminuria. Their NO levels were assayed with NO spin trapping and EPR dosimetry of tissue sections.

Results: compared to controls, diabetic mice have greatly reduced levels of NO in their kidney tissues. EPR spectroscopy shows that Atrasentan largely corrects the bioavailability of NO. In accord, we observe that Atrasentan improves the histological (glycocalyx) and functional (albuminuria) properties of the kidney. Overall, our hypothesis is confirmed.

[1] A. Vanin, A. Huisman, E. van Faassen, *Iron dithiocarbamate as spin trap for nitric oxide detection*, Meth. Enzymol. 359 (2002) 27 – 42

[2] C. Ott et al, *Reduction in basal nitric oxide activity causes albuminuria*, Diabetes 60 (2011) 572 – 576.

Grid-of-errors: a numerical procedure to extract the distribution of magnetic interactions from multi-frequency EPR spectra

Mykhailo Azarkh and Edgar J. J. Groenen

*Huygens-Kamerlingh Onnes Laboratory, Department of Physics, Leiden University,
P.O. Box 9504, 2300 RA, Leiden, The Netherlands
azarkh@physics.leidenuniv.nl*

A proper selection of the microwave frequency increases the resolution of EPR to the extent that the distribution of magnetic interactions becomes apparent. We present an approach called 'grid-of-errors' to extract the distribution of magnetic interactions from continuous-wave EPR spectra at multiple microwave frequencies. This approach is based on the analysis of the lineshape of the spectra and explicitly worked out for high-spin systems for which the lineshape is determined by a distribution of the zero-field splitting. Initial principal values of the zero-field-splitting tensor are obtained from the EPR spectrum at a microwave frequency in the high-field limit, and the initial distribution is taken Gaussian. Subsequently, the grid-of-errors procedure optimizes this distribution, without any restriction to its shape, taking into account spectra at various microwave frequencies. The numerical procedure is illustrated for the Fe(III)-EDTA complex. An optimized distribution of the zero-field splitting is obtained, which provides a proper description of the EPR spectra at 9.5, 34, 94, and 275 GHz (Figure 1). The proposed approach can be used as well for distributions of magnetic interactions other than the zero-field splitting.

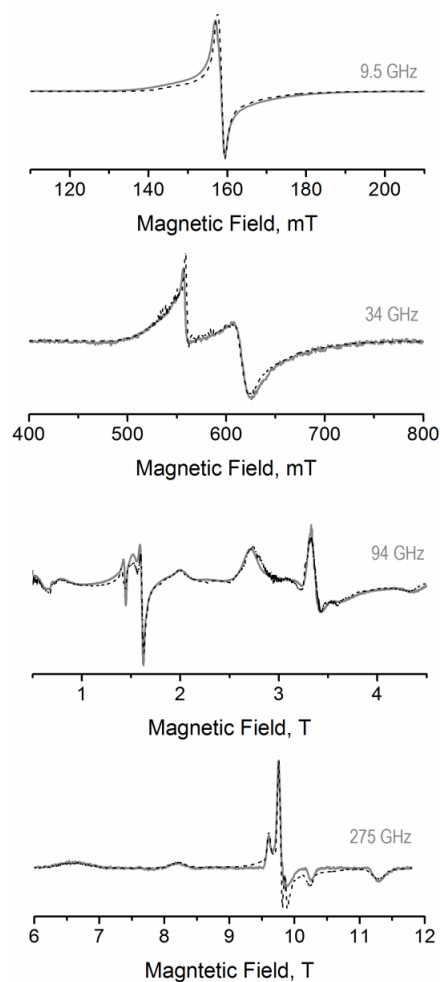


Figure 1. Experimental spectra of Fe(III)-EDTA and simulations (dotted lines), which include the optimized distribution of the zero-field splitting.

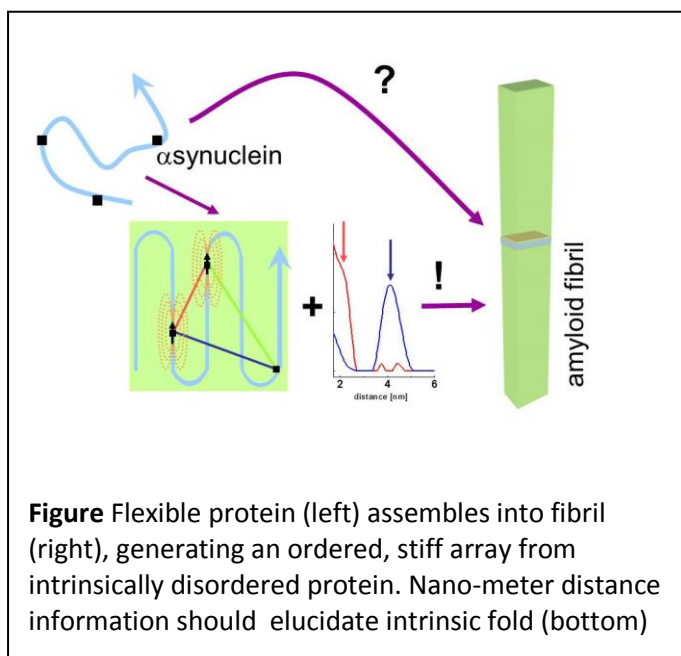
Internal structure of Amyloid-fibrils from EPR long-range distance constraints – possibilities and challenges

Maryam Hashemi Shabestari^[a], Pravin Kumar^[a], Ine M.J. Segers-Nolten^[b], Mireille M.A.E. Claessens^[b], Bart D. van Rooijen^[b], Vinod Subramaniam^{*[b, c]}, and Martina Huber^{*[a]}

^[a]Department of Physics, Huygens-Kamerlingh-Onnes Laboratory, Leiden University, PO Box 9504, 2300 RA Leiden, The Netherlands

^[b]Nanobiophysics, MESA+ Institute for Nanotechnology & ^[c]MIRA Institute for Biomedical Technology and Technical Medicine, University of Twente, PO Box 217, 7500AE Enschede, The Netherlands ^[c] and FOM Institute AMOLF, Science Park 104, 1098 XG Amsterdam, The Netherlands

Amyloid fibrils and plaques are hallmarks of neurodegenerative diseases. Fibrils can be grown *in vitro*, are a few nano-meters in width and can grow to micro-meter length. It is amazing that fibrils, which derive from flexible, often intrinsically disordered proteins, have a stiffness that is close to steel. Knowing the fold of the protein in the fibril would be a first step to understand the assembly process of fibrils.



In Parkinson's disease, plaques (Lewy bodies) consist predominantly of the α -synuclein (α S) protein. Here we determine nm-distance constraints for the protein in the fibril by double electron-electron paramagnetic resonance (DEER) on doubly spin labeled α S-variants, diamagnetically diluted with wild-type α S to suppress intermolecular interactions. Intramolecular distances in three pairs (56/69, 56/90 and 69/90) are reported. An approach to derive a model for the fibril-fold from sparse distance data assuming only parallel β -sheets is described.

Using the distances obtained in this study as input, a model is obtained with three strands, comprising residues 56 to 90, in which the strands consist of eight to twelve residues each. Limitations of the approach are discussed in detail, showing that the interpretation of the data does not yet yield an unambiguous structure model. Possible avenues to improve this situation are described.

Knowledge of the internal architecture of the fibrils should help to understand fibril properties and is essential to understand the processes that occur in neurodegenerative disease.

Abstracts Posters

Impact of erythrocytic eNOS on HbNO formation measured by EPR spectroscopy

F. Dei Zotti, I. Lobysheva, J.L. Balligand

Pole of Pharmacology and Therapeutics, Experimental and Clinical Research Institute, Université Catholique de Louvain, Brussels, Belgium

Introduction: The bioavailability of nitric oxide in circulating blood can reflect the severity of endothelial dysfunction in metabolic and cardiovascular diseases. Therefore a quantitative assay of it is highly desirable. Nitric oxide can form iron-nitrosyl complexes with haemoglobin (5-coordinate- α -HbNO) in erythrocytes (RBCs). Recently RBCs were shown to contain endothelial nitric oxide synthase (eNOS) protein, able to generate and export NO. We developed a modified subtraction method using EPR spectroscopy to quantify HbNO in erythrocytes. We analysed the HbNO level in eNOS^(+/+) and eNOS^(-/-) mouse RBCs and in intact human RBCs under modulation of L-arginine availability *ex vivo*.

Methods and Results: We detected eNOS protein using immunofluorescence microscopy in human and in eNOS^(+/+) mouse RBCs, but it was not detectable in eNOS^(-/-) mouse. We modulated the intraerythrocytic eNOS activity using an inhibitor of NOS (L-NAME) and an inhibitor of arginase (norNOHA) that can compete with eNOS for their common substrate, L-arginine. We studied the influence of L-NAME and norNOHA on the formation of HbNO by EPR measurements, and the accumulation of nitrite and nitrate, potential end products of endogenous NO metabolism in RBCs, using Griess reaction. However, the presence of protein-centred free radicals decreased the quality of the EPR HbNO signal for accurate quantification. It exhibits an EPR signal with g-factor ~ 2.005 and a line width about 19 G that overlapped with the hyperfine structure of HbNO EPR signal. We applied a subtraction method to better discriminate the HbNO that allowed more accurate quantification. We treated mice with or without L-NAME in drinking water for 5 days, then we collected blood, erythrocytes and plasma and we recorded the EPR spectra. In the plasma sample of the mice treated with L-NAME, we observed a protein-centred free radical (FR) component probably generated from free haemoglobin oxidation in the process of hemolysis. We then used this component to perform a digital subtraction to unmask the hyperfine components of HbNO signal in erythrocytes. We determined that the increase in HbNO signal after the addition of norNOHA and L-arginine is prevented by L-NAME. This doesn't occur in eNOS^(-/-) mice highlighting the erythrocytic eNOS activity. We supported these results by the analysis of nitrite and nitrate accumulation in RBCs where we observed that L-NAME, as for the EPR detection procedure, decreased the effect of norNOHA in the accumulation of nitrite and nitrate only in eNOS^(+/+) mice. To determine the influence of NO produced by rat intraerythrocytic eNOS on HbNO level in fresh isolated RBCs, we tested the decay of HbNO after addition of L-NAME *ex vivo*. The HbNO signal from erythrocytes treated with L-NAME at 21% of O₂ was not significantly decreased compared to control erythrocytes, but at 4% of O₂ we observed a small decrease reflecting slight erythrocytic production of NO.

Conclusion: The study demonstrates that intraerythrocytic eNOS is present and has a constitutive activity but the NO produced only minimally influences the whole NO content of erythrocytes suggesting that the bulk of NO reaching circulating erythrocytes comes from endothelial cells.

Preliminary EPR results of the influence of storage temperature on the endogenous antioxidative potential of a widely distributed Belgian pale lager beer

Gauthier Vanhaelewyn⁽¹⁾, Freddy Callens⁽²⁾ and Anita Van Landschoot⁽¹⁾

⁽¹⁾*UGent, Faculty of Bioscience Engineering, Department of Applied biosciences Campus Schoonmeersen, Valentin Vaerwyckweg 1, 9000 Ghent, Belgium*

⁽²⁾*UGent, Faculty of Sciences, Department of Solid State Sciences Sterre Campus, Krijgslaan 281-S1, 9000 Ghent, Belgium*

Abstract

Electron Paramagnetic Resonance (EPR) can be used to predict the flavour-stability in beer by monitoring the so-called lag time. The determination of the lag time is based on the indirect detection, through a spin trap, of the radical generation in beer during forced oxidation (inciting accelerated ageing) at a temperature of 60 °C. Short-lived radicals occur in beer most likely due to oxidation products of metal ions present in beer, mainly originating from wort. For a specific period of time, these radicals are annealed by the endogenous anti-oxidative compounds in beer. When these compounds are depleted the amount of radicals in beer increases rapidly with time causing ageing of the beer.

In this poster we present preliminary EPR results on the change of lag time of a bottled widely distributed Belgian pale lager beer stored at elevated temperatures (32°C and 37°C). Monitoring the variation of the lag time over time using EPR offers a tool to quantitatively estimate its flavor-stability. The different lag times, as a function of storage time, were deduced from the magnitude of the EPR signals induced by the spin-trap *N-tert-Butyl- α -(4-pyridyl)nitron N'-oxide* (POBN) during forced oxidation. A rapid decrease in lag time with a time constant of about 4 days has been observed for the beer stored at the aforementioned elevated temperatures. This indicates, among other factors, the relevance of adequate storage temperatures.

Multi-frequency EPR spectroscopy of Eu^{2+} –activated persistent luminescent materials

E. Gabriele Panarelli, Peter Gast, Edgar J. J. Groenen

*Leiden University, Dept. of Physics, Huygens-Kamerlingh Onnes Laboratory
P.O. Box 9504, 2300 RA Leiden, The Netherlands*

Ever since the first 1996 report by Matsuzawa et al. on the persistent luminescence properties of $\text{SrAl}_2\text{O}_4:\text{Eu}^{2+},\text{Dy}^{3+}$ [1], this and other europium(II)-activated lanthanide-co-doped alkaline-earth aluminates have been attracting much attention because of their outstandingly long afterglow (in some cases even over 30 hours), of their tunability of emission, and of their high chemical stability. Main applications have been developed in emergency lighting, safety signage, and bio-imaging [2].

So far though, no mechanism has been found that could conclusively explain how luminescence arising from Eu^{2+} (the activator ion) can be dramatically delayed in time upon co-doping with Dy^{3+} or other trivalent lanthanides to give persistent luminescence. Several mechanisms have appeared in the literature [3] [4] [5], and albeit often contradictory, they show general consensus over the fact that photoexcited electrons from europium's 4f to 5d levels are trapped somewhere in the host lattice. Subsequently, these trapped electrons are thermally released back to europium, where a photon is emitted upon electron relaxation. The thermal release, being exponentially dependent on the traps' energy depth, takes place slowly at room temperature, leading to persistent luminescence (i.e. delayed light emission).

Anyway, the chemical nature of the traps remains unknown, though most researchers agree that oxygen vacancy traps ($\text{VO}^{\cdot\cdot}$ or VO^{\cdot}) should be involved. By means of both continuous-wave and pulsed multi-frequency Electron Paramagnetic Resonance (95 and 275 GHz), we aim at detecting paramagnetic photogenerated traps and photo-induced modifications of the ground-state $S = 7/2$ Eu^{2+} spectrum. Such modifications might thus provide insights into the afterglow mechanism for this class of phosphors.

[1] T. Matsuzawa et al., J. Electrochem. Soc., **1996**, 143, 2670-2673.

[2] K. Van den Eeckhout et al., Materials, **2010**, 3, 2536-2566.

[3] P. Dorenbos, J. Electrochem. Soc., **2005**, 152, H107-H110.

[4] F. Clabau et al., Chem. Mater., **2005**, 17, 3904-3912.

[5] T. Aitasalo et al., J. Phys. Chem. B, **2006**, 110, 4589-4598.

Characterization of Class 1 hemoglobins from the model legume *Lotus japonicus* using EPR and optical spectroscopy

B. Cuypers*¹, L. Calvo², M. Becana², and S. Van Doorslaer¹

¹*BIMEF Laboratory, Department of Physics, University of Antwerp, Universiteitsplein 1, 2610 Wilrijk, Belgium*

²*Departamento de Nutrición Vegetal, Estación Experimental de Aula Dei, Consejo Superior de Investigaciones Científicas, Apartado 13034, 50080 Zaragoza, Spain*

**bert.cuypers@uantwerp.be*

Hemoglobins (Hbs) are widespread in all kingdoms of life. In plants, there are three distinct types of Hbs: symbiotic, nonsymbiotic, and truncated Hbs. Nonsymbiotic plant hemoglobins are typically found at submicromolar concentrations and are divided into two classes. Class 1 Hbs display an extremely high affinity for oxygen and are induced in hypoxic conditions, while Class 2 Hbs have a lower oxygen affinity and are induced by a low temperature.¹ The model legume *Lotus japonicus* expresses three symbiotic Hbs (leghemoglobins), three nonsymbiotic Hbs (two of class 1 and one of class 2), and two truncated or class 3 Hbs.² In this work, we characterize the ferric form of the two class 1 Hbs that are expressed in *L. japonicus* using Electron Paramagnetic Resonance (both continuous-wave and pulsed) and Resonance Raman Spectroscopy. All the obtained spectra are compared with those of published data available for other plant class 1 Hbs. The proteins were found to be in a low-spin ($S = 1/2$) hexacoordinated form, as is expected for class 1 Hbs. The ¹⁴N hyperfine and nuclear quadrupole tensors, as obtained by HYSCORE and 3-pulse-ESEEM experiments and simulations, indicate a different orientation of the His imidazole planes when compared to tomato hemoglobin (SOLly GLB1).

¹M. Perazzolli, P. Dominici, M.C. Romero-Puertas, et al., "Arabidopsis nonsymbiotic Hemoglobin AHb1 modulates nitric oxide bioactivity," *Plant Cell.*, 16, 2785-2794, 2004.

²P. Bustos-Sanmamed, A. Tovar-Méndez, M. Crespi, et al., "Regulation of nonsymbiotic and truncated hemoglobin genes of *Lotus japonicus* in plant organs and in response to nitric oxide and hormones," *New Phytol.*, 189,765-776, 2010.

Processing-induced near-interfacial thermal donor generation in (100)Si/Si-oxycarbide insulator structures revealed by electron spin resonance

S. Iacovo, A. Stesmans, S. Nguyen, and V. V. Afanas'ev

Semiconductor Physics Laboratory, Department of Physics, University of Leuven, 3001 Leuven, Belgium

Low temperature electron spin resonance (ESR) study of Cz-(100)Si/insulator structures with organosilicate films of low dielectric constant κ grown at 300 °C using plasma-enhanced chemical vapor deposition (PECVD) reveals, after subjection to UV-irradiation assisted thermal curing at 430 °C to remove organics, the observation of the NL8 ESR spectrum. This indicates the generation in the c-Si substrate of singly ionized thermal double donor (TDD) defects with a core contained of oxygen atoms. The generation is found to be highly non uniform, which is concluded to be the result of interfacial stress acting as the major driving component in the enhancement of TDD formation during thermal treatment. This suggests substantial stress being involved with PECVD organosilicate low- κ glasses.

Effect of laser excitation intensity on the spin-dependent NV⁻ fluorescence in diamond

Shashi K. R. Singam,¹ Miloš Nesládek,³ Michele Giugliano,² Etienne Goovaerts¹

¹*Experimental Condensed Matter Physics, Physics Department, and* ²*Theoretical Neurobiology and Neuroengineering, Department of Biomedical Sciences, University of Antwerp, Belgium.*

³*Hasselt University, Institute for Materials Research (IMO), University of Hasselt, Belgium*

The charge state NV⁻ of the nitrogen-vacancy center in diamond displays a fluorescence efficiency depending on the spin state in the triplet ground level, of particular interest for various applications. The NV⁻ fluorescence can be influenced in ambient conditions either by microwave excitation or by an applied static magnetic field. For application in background-free fluorescence microscopy [1-3] it is important to consider that the induced contrast is strongly dependent on laser excitation intensity. We present measurements of the microwave-induced and field-induced contrast in NV⁻ fluorescence in both an HPHT grown (100) oriented diamond single crystal and for fluorescent nanodiamonds (FNDs) over 6 orders of magnitude variation of the optical excitation density. Field-induced contrasts of up to 37% are observed in the single crystal under intense excitation. Microwave-induced contrast is relatively low and also decreasing at high optical excitation densities. For better analysis of the data, model calculations were performed in both cases. Understanding the detailed characteristics in the two approaches allows for an optimal choice of method and conditions depending on the requirement of the specific application.

[1] R. Igarashi, et al, Nano Lett. 2012, 12, 5726-5732.

[2] A. Hegyi, E. Yablonovitch, Nano Lett. 2013, 13, 1173-1178.

[3] R. Chapman, T. Plakhoitnik, Opt. Lett. 2013, 38, 1847-1849.

Electron paramagnetic resonance and fluorescence studies on potential anticancer properties of two new Ru(II) complexes : preliminary results

Collienne S.¹, Hoebeke M.¹, Terrak M.², Mouithys-Mickalad A.³, Delaude L.⁴

1. *Laboratory of Biomedical Spectroscopy, University of Liège, Belgium*

2. *Centre of Protein Engineering (CIP), University of Liège, Belgium*

3. *Centre for Oxygen, R&D (CORD), University of Liège, Belgium*

4. *Laboratory of Organometallic Chemistry and Homogeneous Catalysis, University of Liège, Belgium*

Fight against cancer is a priority of today's research. According to WHO¹, more or less 10 million people died every year because of this disease. Since the discovery of the anticancer properties of cisplatin (CisPt) in 1965 by Rosenberg [1], the treatment of cancer by chemotherapy has known great improvements. Unfortunately, CisPt has several side effects and is not effective against all kinds of cancer. Nevertheless its use highlights the great potential of organometallic compounds in the treatment of cancer [2]. Here we investigated the potential anticancer properties of two new organometallic compounds based on ruthenium II : $[RuCl(p\text{-cymene})(S_2C.IDip)]^+(PF_6)^-$ and $[RuCl(p\text{-cymene})(S_2C.Icy)]^+(PF_6)^-$ named as LDO436 and LDO437 respectively.

The cytotoxicity of the Ru-complexes and CisPt on keratinocyte (HaCat) cell line was determined by MTT assay. LDO437 shows higher cytotoxicity than LDO436 and both were found much higher than CisPt. In order to understand the mechanism of action leading to cell death, Electron Paramagnetic Resonance (EPR) combined with the spin labelling technique was used to measure the membrane microviscosity and a "hypothetical" membrane perturbation of the Ru-complexes as a cause of the cancer cells death. EPR results show no variation of membrane microviscosity and led us to rethink our first hypothesis.

CisPt is a well-known DNA-interacting molecule and the current thinking is that the inhibition of DNA replication is an essential first step of the cytotoxicity of the organometallic compound [3]. To gain more information, we are planning to investigate the DNA-interaction properties of the Ru-complexes using fluorescence spectroscopy as well as their antioxidant properties by EPR and spin trapping methods.

References:

1. Nafees M., Zijian G., *Current Opinion in Chemical Biology* (2014), 144-153.
2. Dasari S., Tchounwou P., *European Journal of Pharmacology* 740 (2014), 364-378.
3. Gonzalez V., Fuertes M., Alonso C., Perez J., *Mol Pharmacol* 59 (2001), 657-663.

¹World Health Organization

Electron magnetic resonance study of radiation-induced radicals in DNA

J. Kusakovskij, F. Callens, H. Vrielinck

Ghent University, Department of Solid State Sciences, Krijgslaan 281-S1, B-9000 Ghent, Belgium

It is widely known that free-radical-mediated damage to biomolecules brings dire consequences to living organisms. In the context of high energy radiation effects on DNA, neutral sugar radicals are very important because of their links to strand breaks – the main actors in radiation induced mutation and carcinogenesis [1]. Considerable progress has been made in understanding the radical composition of irradiated DNA by studying it directly or by examining model systems [2]. Most of the identification relied on comparisons of isotropic HF interactions to DFT calculations, so chemical structures of radicals are still somewhat ambiguous. It is not unreasonable to assume that some of these ambiguities would be solved if anisotropic data was acquired by employing more advanced EPR techniques, like multifrequency EPR spectroscopy or hyperfine selective EPR techniques (ENDOR, e.g.).

In this contribution we present the first results of our work, finally aiming at studying neutral sugar radicals in irradiated DNA with ENDOR. After low temperature (80 K) irradiation the EPR spectrum of DNA is known to be dominated by charged base radicals: e^-/h^+ scavengers ($K_3Fe(CN)_6/K_4Fe(CN)_6$) have to be employed to suppress their formation [3]. Variations of the Q band (34 GHz) EPR spectrum using different combinations of scavengers (see Fig. 1) were recorded and compared to literature X-band results. Temperature scans of EPR and matrix ENDOR spectra will also be presented and discussed.

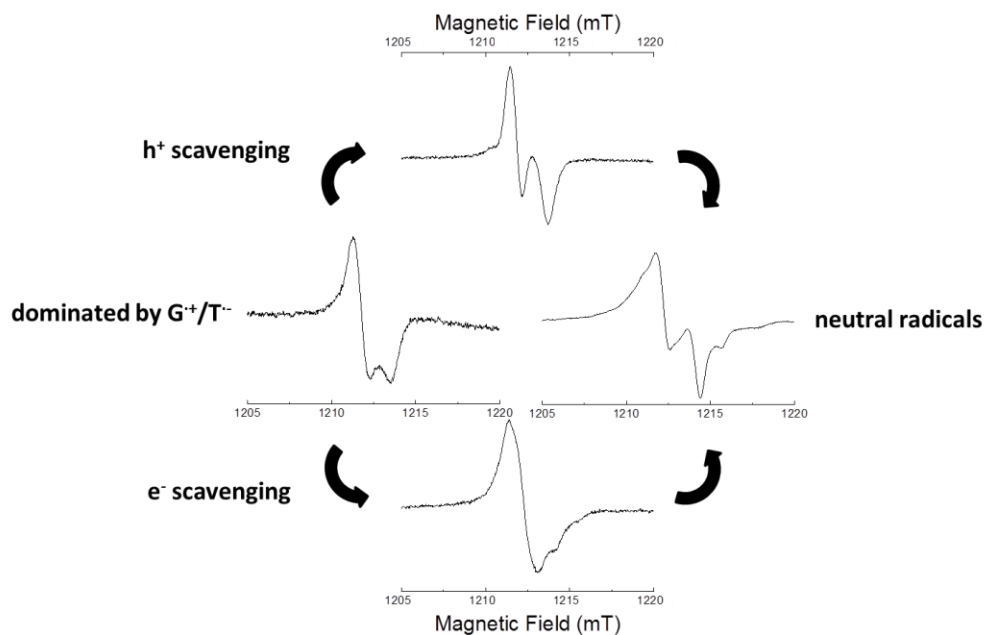


Figure 1: Scheme illustrating the effect of hole and electron scavengers to X-irradiated DNA.

1. von Sonntag, C. Free-Radical-Induced DNA Damage and Its Repair; Springer-Verlag: Berlin, Heidelberg, 2006; pp 335–447.
2. Adhikary, A.; Becker, D.; and Sevilla, M.D. In Applications of EPR in Radiation Research; Lund, A., Shiotani, M., Eds.; Springer International Publishing, 2014; pp 304-352.
3. Shukla, L. I.; Pazdro, R.; Becker, D. and Sevilla, M. D. Radiation Research (163) 2005; 591–602.

Ghent University

Freddy Callens

Kristof Daelman

Jevgenij Kusakovskij

Wouter Leroy

Kwinten Maes

Irena Nevjestic

Johan Van Driessche

Gauthier Vanhaelewyn

Henk Vrielinck

Freddy.Callens@UGent.be

Kristof.Daelman@UGent.be

Jevgenij.Kusakovskij@UGent.be

Wouter.Leroy@UGent.be

Kwinten.Maes@UGent.be

Irena.Nevjestic@UGent.be

Johan.VanDriessche@UGent.be

Gauthier.Vanhaelewyn@UGent.be

Henk.Vrielinck@UGent.be